

Full Length Research Paper

A systematic procedure for analysis of third-order charge pump phase-locked loop (PLL)

Habib Adrang

Nour Branch, Islamic Azad University, Nour, Iran. E-mail: hadrang@gmail.com.

Accepted 24 August, 2011

This paper represents a simple and easy to learn method for analysis and design of third-order charge pump phase-locked loop (PLL) and provides analytical equations for calculating the desired specifications such as phase margin (PM), damping ratio and small signal settling time. The proposed method is based on dominant pole approximation. In other words, this method is based on the approximation of the transfer function of the third-order PLL through transfer function as a second order system. The validity of the obtained analytical equations has been verified in two examples. Simulation results of the introduced method demonstrate precision in designed parameters.

Key words: Charge pumps phase-locked loop (PLL), phase detector, phase margin (PM), settling time, damping ratio, natural frequency.

INTRODUCTION

Phase-locked loops (PLLs) are widely used in high speed data communication systems. They are generally used for clock recovery and frequency synthesizing of wireless communication systems. The most desirable features of a PLL in high speed communication systems are stability characteristics, fast locking time, low power, small area and immunity to process, voltage, and temperature (PVT) variations (Yin et al., 2011). For example, a wider loop bandwidth is directly translated to a faster locking, and hence, the bandwidth must be maximized to minimize lock time. There are a great number of papers devoted to analysis and design of second-order charge pump PLL (Ping-Hsuan et al., 2011; Monterio et al., 2004; Carlosena et al., 2008; Carlosena and Lazaro, 2006; Gardner, 1980; You and He, 2004; Lakshmikummar, 2009; Woo et al., 2008; Razavi, 2001). But, the existing methods are not efficient in analysis of higher order architectures such as type II third-order PLL because there is an additional pole in transfer function that degrades the phase margin (PM) and causes peaking in the frequency response. Therefore, finding an analytical

approach for the designing of the third-order PLLs is still a topic of interest among researchers. Hence, in this work we tried to produce a method for finding the optimal location of the third pole and introduce analytical equations for designing the system specifications such as PM and damping ratio. The frequency domain analysis of third-order PLLs has been presented in different papers (Carlosena et al., 2008; Carlosena and Lazaro, 2006; Gardner, 1980) but, the transient analysis has not been investigated. The equations governing the third-order PLL have been extracted in (You and He, 2004) but, there is not any method for the designing of important specifications in it. In this paper, a simple and easy to understand method is introduced for analysis of the third-order PLL. In the proposed method, the close-loop transfer function of the third-order PLL is approximated through a second-order transfer function using the dominant pole approximation. It is relatively easy to design a PLL with the given specifications using the proposed procedure and the design can then be evaluated using computer simulation.

Third-order charge pump phase-locked loop (PLL)

Abbreviations: PLL, Phase-locked loop; PVT, process, voltage, and temperature; PFD, phase frequency detector; VCO, voltage controlled oscillator; PM, phase margin.

There are several structures of PLLs and most of the presented architectures are based on charge pump. A

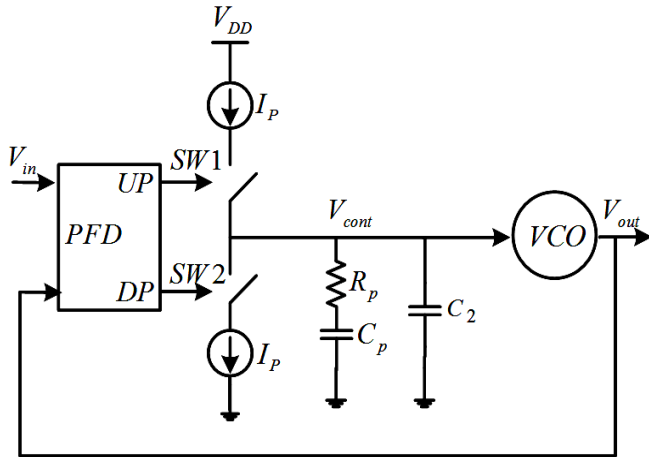


Figure 1. Structure of the third-order charge pump PLL.

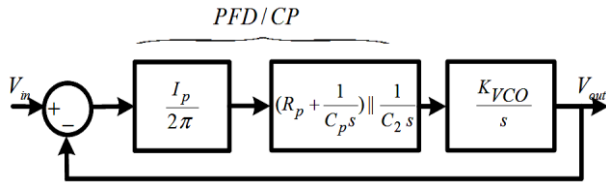


Figure 2. Systematic model of the third-order charge pump PLL.

conventional charge pump third-order PLL consists of phase frequency detector (PFD), charge pump, loop filter and the voltage controlled oscillator (VCO). A charge pump consists of two switched current sources that pump charge into or out of the loop filter. The structure of the PLL and its systematic model, are shown in Figures 1 and 2, respectively.

The PFD compares the phase or frequency difference between the input (V_{in}) and output (V_{out}) signals and generates an error signal. Then, the charge pump converts the error signal pulses into analog current pulses. The analog current mode pulses are then integrated and converted to a voltage V_{cont} through the loop filter. Also, the noise and the high frequency components at the output of the charge pump will be removed by the loop filter which includes R_p , C_p and C_2 . The resulted integrated signal at the output of the loop filter drives the VCO which generates a signal with a specific frequency depending on its input voltage. Here, C_2 is used to suppress the sudden jump on the VCO control voltage due to charge injection and clock feed through SW_1 and SW_2 in V_{cont} also improves the transient characteristics. This additional capacitance increases the PLL order to three. The open loop transfer function of this third-order type II PLL is shown in Equation 1.

$$H(s)|_{open} = \frac{I_p K_{VCO}}{2\pi(C_2 + C_p)} \frac{R_p C_p s + 1}{s^2 \left[\frac{R_p C_p}{b} s + 1 \right]} = K_v \frac{R_p C_p s + 1}{s^2 \left[\frac{R_p C_p}{b} s + 1 \right]} \quad (1)$$

Where, K_{VCO} is the VCO gain, I_p is the charge pump current, $b=1+C_p/C_2$, and $K_v=I_p K_{VCO}/[2\pi(C_2+C_p)]$.

In the first step, the PM is calculated. To determine the PM, the magnitude of the open loop gain has been plotted with respect to frequency ω and the crossover frequency (ω_{PM}) has been determined. Bode diagram of the magnitude and phase of the third-order PLL for the stability analysis is shown in Figure 3. From Figure 3, we obtain:

$$\frac{x_1}{\log(1/R_p C_p)} = 40 \quad (2)$$

$$\frac{x_2}{\log(\omega_{PM}) - \log(1/R_p C_p)} = 20 \quad (3)$$

Knowing that $x_1+x_2=20\log K_v$, the crossover frequency will be given by:

$$\omega_{PM} = \frac{I_p K_{VCO}}{2\pi(C_2 + C_p)} (R_p C_p) = K_v (R_p C_p) \quad (4)$$

$$\angle H|_{open} = -180 + \tan^{-1}(R_p C_p \omega) - \tan^{-1}\left(\frac{R_p C_p}{b} \omega\right) \quad (5)$$

Furthermore, the PM equals:

$$PM = \tan^{-1}(R_p C_p \omega_{PM}) - \tan^{-1}\left(\frac{R_p C_p}{b} \omega_{PM}\right) \quad (6)$$

As shown in Figure 3, by decreasing K_v , the crossover frequency moves toward the origin and this degrades the PM. Assuming that $X=R_p C_p \omega_{PM}$, Equation 6 can be rewritten as:

$$\tan(PM) = \frac{(1-1/b)X}{1+(X^2/b)} \quad (7)$$

The PM will be maximized if the first derivative with respect to X is set to zero. As a result, the maximum PM will be achieved when:

$$X = R_p C_p \omega_{PM} = \sqrt{b} \quad (8)$$

Substituting this value of X in Equation 7, it will be obtained that:

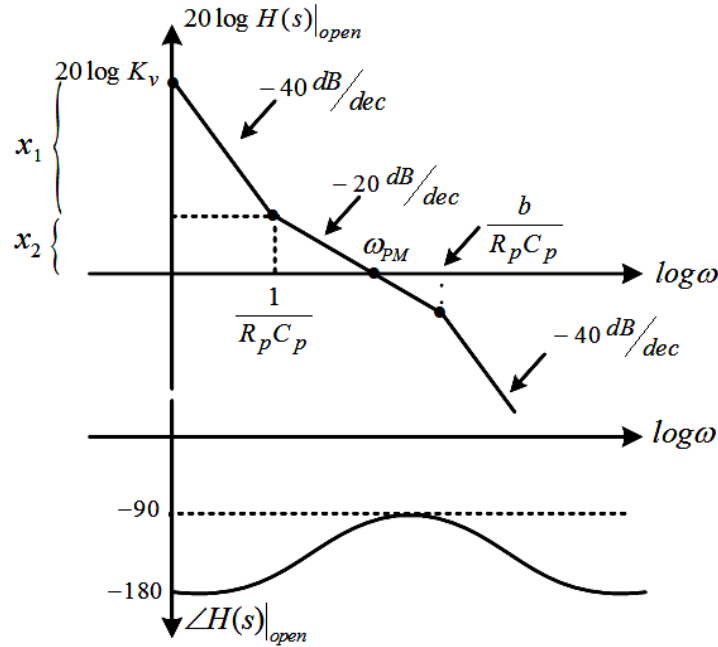


Figure 3. Bode plots open loop transfer function of the PLL.

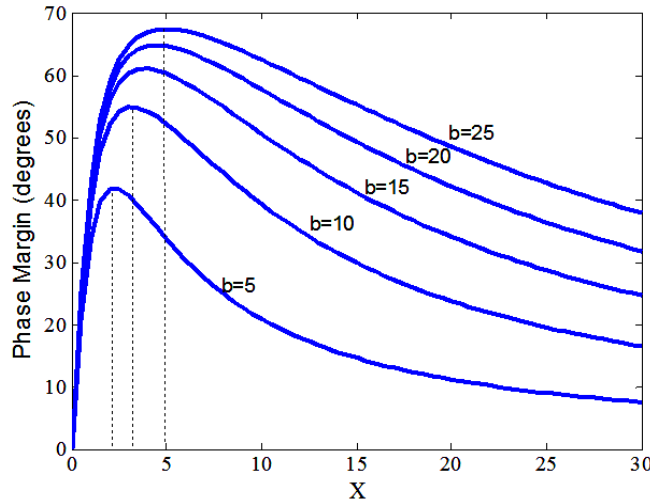


Figure 4. Phase margin as a function of $X=R_pC_p\omega_{PM}$.

$$\tan(PM|_{\max}) = \frac{1}{2} \left(\frac{b-1}{\sqrt{b}} \right)$$

$$\Rightarrow PM|_{\max} = \tan^{-1} \left[\frac{1}{2} \left(\frac{b-1}{\sqrt{b}} \right) \right] \tag{9}$$

Thus, the maximum PM is only a function of b or the ratio of C_p to C_2 . In Figure 4, the phase is plotted against margin as a function of X. As shown, the PM will be

maximized when $X = \sqrt{b}$. On the other hand, for a given value of b if Equation 8 is satisfied, the maximum PM will be calculated from Equation 9. Therefore, the PM can be increased by increasing b or the ratio C_p/C_2 . For example, assuming $b=20$, maximum available PM is 64.8° . Substituting Equation 4 in Equation 8, we have:

$$K_v(R_pC_p)^2 = \sqrt{b} \tag{10}$$

Roots locus analysis and proposed approach

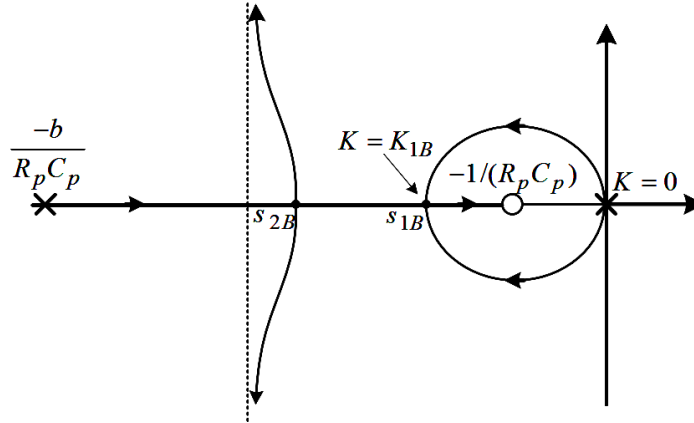


Figure 5. Roots locus plot for type II third-order PLL.

The open loop transfer function of a type II third-order PLL can be rewritten as:

$$H(s)|_{open} = \frac{I_p K_{VCO}}{2\pi(C_2 + C_p)} \frac{R_p C_p s + 1}{s^2} = \frac{I_p K_{VCO}}{2\pi C_2} \frac{s + \frac{1}{R_p C_p}}{s^2 \left[\frac{b}{s + \frac{b}{R_p C_p}} \right]} = K \frac{s + z}{s^2 (s + p)} \quad (11)$$

Where, $z = 1/(R_p C_p)$, $p = b/(R_p C_p) = bz$ and $K = I_p K_{VCO} / (2\pi C_2)$. By comparing K and K_V :

$$K = K_V b \quad (12)$$

Substituting Equations 4 and 12 in Equation 8 gives the following equation:

$$K(R_p C_p)^2 = b\sqrt{b} \\ \Rightarrow K = K_{PM\max} = b\sqrt{b}.z^2 \quad (13)$$

The parameter $K_{PM\max}$ is the desired gain to achieve the maximum PM. Figure 5 shows the roots locus plot of the type II third-order PLL as a function of K.

As depicted in Figure 5, for $K=0$ in $s=0$ to $K=K_{1B}$ in break point ($s=s_{1B}$), the roots are complex and damping ratio (ξ) varies between 0 and 1. For adjusting damping ratio ($0 \leq \xi \leq 1$), K should be less than or equal to K_{1B} therefore we must determine the value of K_{1B} . The closed loop characteristic equation is required for calculating the break point (s_{1B}).

$$1 + K \frac{s + z}{s^2 (s + p)} = 0 \Rightarrow K = -\frac{s^2 (s + p)}{s + z} \quad (14)$$

In order to determine the break points, the roots of $dK/ds=0$ should be calculated.

$$s^2 + \frac{1}{2}(3z + p)s + p.z = 0 \quad (15)$$

In Equation 15, $p=bz$, therefore, by solving it, we have:

$$s^2 + \frac{1}{2}(b + 3)s + b.z^2 = 0 \\ \Rightarrow s_{1,2B} = -\frac{1}{4}z \left[(b + 3) \pm \sqrt{(b - 1)(b - 9)} \right] \quad (16) \\ \Rightarrow s_{1B} = -\frac{1}{4}z \left[(b + 3) - \sqrt{(b - 1)(b - 9)} \right] = -\beta z$$

Where, $\beta = -0.25 \left[(b + 3) - \sqrt{(b - 1)(b - 9)} \right]$. Knowing that $s_{1, 2B}$ are real, thus $b \geq 9$. Substituting s_{1B} from Equation 16 into Equation 14, K_{1B} can be calculated as:

$$K_{1B} = \frac{\beta^2 z^2 (b - \beta)}{\beta - 1} \quad (17)$$

If Equation 13 is satisfied, PM will be maximized. Moreover, in order to adjust damping ratio between 0 and 1, the following condition must be satisfied:

$$K = K_{PM\max} = b\sqrt{b}.z^2 \leq K_{1B} = \frac{\beta^2 z^2 (b - \beta)}{\beta - 1} \quad (18) \\ \Rightarrow b\sqrt{b} \leq \frac{\beta^2 (b - \beta)}{\beta - 1}$$

Equation 18 is used to plot Figure 6 as a function of b. Numerical computation and Figure 6 show that Equation 18 is true only for minimum value of b that is $b = 9$ and from Equation 9, $PM_{\max} = 53^\circ$. This means that if Equation 13 is satisfied and $b > 9$ then, $K > K_{1B}$ and all poles of the closed loop system become real and the damping ratio

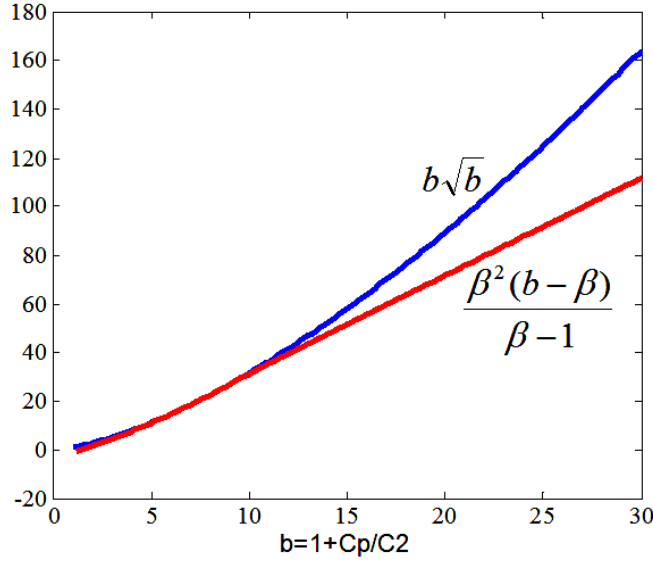


Figure 6. Plots to compare Equation 18.

will always be equal to 1. Therefore, we cannot simultaneously maximize PM and adjust ξ for desired settling time or bandwidth. This implies that there is a trade-off between the maximum PM and damping ratio. In this paper, a technique is introduced to adjust b , ξ and PM simultaneously. The design can be evaluated using computer simulation.

Analysis of the closed loop system

Beside the open loop response, it is also needed to analyze the closed loop response from which two major factors can be calculated: damping ratio, and natural frequency. In order to have a faster locking time, usually the damping factor should approach 1, and the natural frequency should be smaller than one tenth of the input frequency (You and He, 2004). The closed loop transfer function of the third-order PLL described above is given as:

$$H(s)|_{close} = \frac{\frac{K_v b}{R_p C_p} (R_p C_p s + 1)}{s^3 + \frac{b}{R_p C_p} s^2 + K_v b s + \frac{K_v b}{R_p C_p}} \tag{19}$$

Assuming that, $0 \leq K \leq K_{1B}$ and considering the roots locus plot, the closed loop system has one real pole and two conjugate complex poles. Therefore, the denominator of Equation 19 can be written as:

$$\begin{aligned} & (s^2 + 2\xi\omega_n s + \omega_n^2)(s + \alpha) \\ &= s^3 + (2\xi\omega_n + \alpha)s^2 + (\omega_n^2 + 2\xi\omega_n\alpha)s + \omega_n^2\alpha \tag{20} \\ &= s^3 + \frac{b}{R_p C_p} s^2 + K_v b s + \frac{K_v b}{R_p C_p} \end{aligned}$$

Where, ω_n and α are the natural frequency and real pole of the closed-loop system, respectively. Also, Figure 7 shows the pole-zero placement of the closed-loop system. Using Equation 20 we have:

$$\begin{cases} \omega_n^2 \alpha = \frac{K_v b}{R_p C_p} = K z \\ \omega_n^2 + 2\xi\omega_n \alpha = K_v b = K \\ 2\xi\omega_n + \alpha = \frac{b}{R_p C_p} = b z \end{cases} \tag{21}$$

To approximate this third-order system by a second-order system, the dominant pole approximation is used. In this work, the ratio $\alpha/\xi\omega_n$ should be greater than 5 or 10. In this condition, we can write $\alpha = m\xi\omega_n$ for $m \geq 5$. Substituting α in Equation 21 we have:

$$\begin{cases} m\xi\omega_n^3 = \frac{K_v b}{R_p C_p} = K z \\ (1 + 2m\xi^2)\omega_n^2 = K_v b = K \\ (2 + m)\xi\omega_n = \frac{b}{R_p C_p} = b z \end{cases} \tag{22}$$

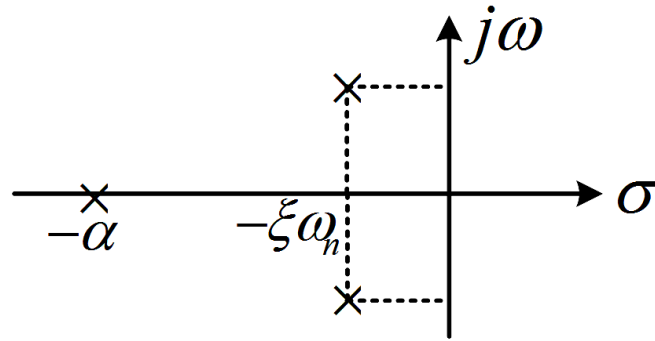


Figure 7. Pole-zero placement of the closed loop system.

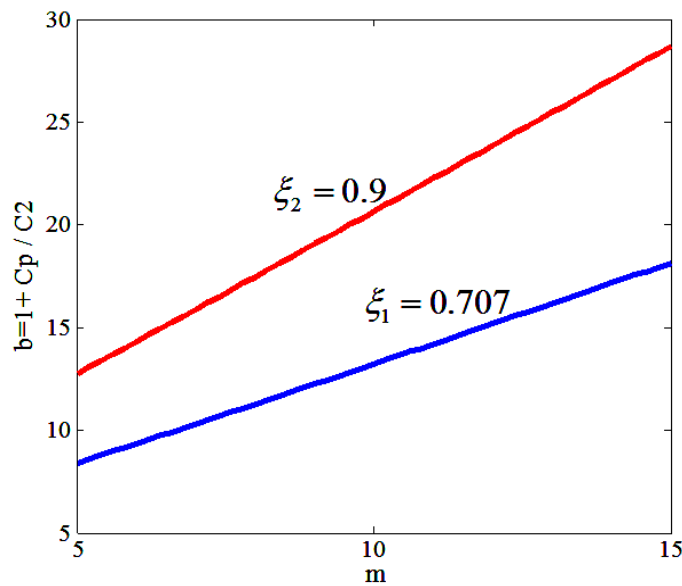


Figure 8. Variation of 'b' as a function of 'm' for ξ1=0.707 and ξ2=0.9.

Equation 22 results:

$$\xi\omega_n = \frac{1+2m\xi^2}{m} \frac{1}{R_p C_p} \tag{23}$$

$$b = (1 + \frac{2}{m})(1 + 2m\xi^2) \tag{24}$$

$$K = \frac{mb^3 z^2}{(2+m)^3 \xi^2} \tag{25}$$

Therefore, the PLL parameters are calculated from Equations 23 to 25. Meanwhile, Figure 8 shows the variation of b in terms of m for two different values of ξ. As it can be seen, b will be increased by increasing the m

value. Equation 24 helps us to determine b.

According to Equation 23, ξω_n will be decreased by increasing the m, R_p and C_p values. Moreover, since t_s is proportional to 1/(ξω_n) (Lakshmikummar, 2009), the small signal settling time will be decreased. Thus, we should not select large values for m, R_p and C_p. On the other hand, this approximation is correct while K ≤ K_{1B}. In other words:

$$\frac{mb^3}{(2+m)^3 \xi^2} \leq \frac{\beta^2(b-\beta)}{\beta-1} \tag{26}$$

Design rules and simulation results

In order to investigate the validity of the proposed approach, two interesting examples of the parameter adjustments for given damping ratio are presented and

Table 1. Parameters for two examples (previous simulation).

	Example1	Example 2
Damping ratio (ξ)	0.707	0.9
b	13.2	20.6
C_p (pf)	12.2	12.2
C_1 (pf)	1	0.6
R_p (K Ω)	10	10
I_p (μ A)	562	791
ω_n (Mrad/s)	12.7	15.6
ω_{PM} (Mrad/s)	16.5	24
PM(degree)	56°	63°

Table 2. Equation 26 condition for the two examples.

	Example1	Example 2
$f_1 = \frac{mb^3}{(2+m)^3 \xi^2}$	26.62	62.46
$f_2 = \frac{\beta^2(b-\beta)}{\beta-1}$	44.35	74.16
$f_1 \leq f_2$	ok	ok

simulated here.

Example 1

The design is started to reach $\xi_1=0.707$. Since, larger values of b lead to greater PM, $m=10$ is selected and according to Equation 24, we have $b=13.2$ and $C_p/C_1=12.2$. With this value of b, using Equation 9, PM will be undoubtedly less than 59°. Assuming $C_1=1$ pf, then $C_p=12.2$ pf. Also, if $R_p=10$ K Ω then using Equation 23, $\omega_n=12.7$ Mrad/s. The subsequent step is calculation of the I_p value. Assuming $K_{VCO}=20 \times 10^6$ Hz/V (Carlosena and Lazaro, 2006) (usual value of K_{VCO}), based on Equations 11 and 25, we can write:

$$K = \frac{mb^3 z^2}{(2+m)^3 \xi^2} = \frac{I_p K_{VCO}}{2\pi C_1} \quad (27)$$

So, $I_p=562\mu$ A. Eventually from Equation 4, $\omega_{PM}=16.5$ Mrad/s and using Equation 7, PM =56°. Equation 23 implies that the settling time will be reduced if R_p becomes small. But it will increase the power consumption significantly because according to Equation 27, if R_p is decreased by a factor of n and other parameters are fixed, I_p should be increased by a much larger factor of n^2 to reach same specifications. For example, if $R_p=1$ K Ω , then I_p will be 100 times higher (56.2

mA) and this value is very large.

According to Equation 27, if K_{VCO} is increased, we can select smaller I_p and R_p . This causes reduction in the power consumption and the settling time. A wide tuning rang VCO with larger values of K_{VCO} has been proposed in Kim et al. (2008) and Nakamura et al. (2006)

Example 2

Now, the design procedure for $\xi_2=0.9$ is presented. For $m=10$ we have $b=20.6$, similar to the previous example, $C_1=1$ pf and $C_p=35.7$ pf. From Equation 23, by increasing the C_p value, $\xi\omega_n$ will be reduced and t_s will be increased and this is not desirable (Yin et al., 2011). Hence, similar to the pervious example, we choose $C_p=12.2$ pf therefore, $C_1=0.6$ pf. Also, if $R_p=10$ K Ω , using Equation 23, $\omega_n=15.6$ Mrad/s. As a result from Equation 27, $I_p=791$ μ A. Finally from Equation 4, $\omega_{PM}=24$ Mrad/s and according to Equation 7, PM=63°. Table 1, summarizes the parameters of the two examples.

Note that as discussed above, the design is valid only when the Equation 26 condition is satisfied. Table 2 depicts the Equation 26 condition for the two examples. In order to determine the precision of the introduced approach, the frequency response and also the step response of the former examples have been simulated in MATLAB and are demonstrated in Figures 9 and 10, respectively. The results of the two examples are

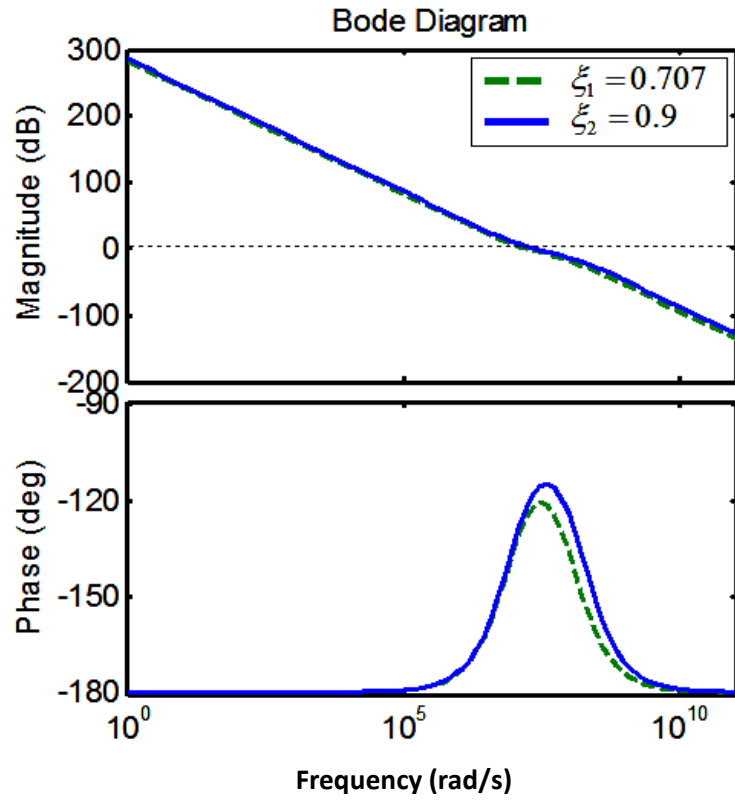


Figure 9. The frequency responses for $\xi_1=0.707$ and $\xi_2=0.9$.

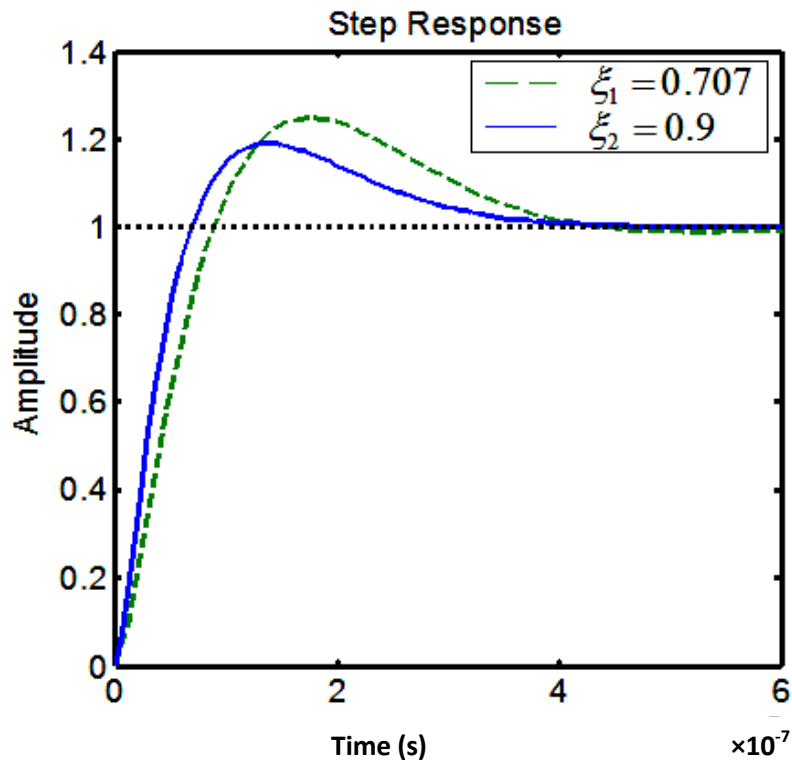


Figure 10. The step responses for $\xi_1=0.707$ and $\xi_2=0.9$.

Table 3. Simulation results for $\xi_1=0.707$, $\xi_2=0.9$ and $m=10$.

After simulation	Example 1	Example 2
Damping ratio (ξ)	0.707	0.88
Rise Time (ns)	64	49
Settling Time (ns)	392	351
Overshoot	24%	18%
m	10	10.5
ω_n (Mrad/s)	12.8	15.3
ω_{PM} (Mrad/s)	18	25
PM(degree)	56°	63°

compared in Table 3. The simulations show the exact agreement between the simulation results and the results from the proposed approach for analysis and design.

CONCLUSION

A systematic method for analysis and design of the third-order charge pump PLL has been presented. In the presented analysis procedure, the results obtained for second-order PLL has been used as an approximation in the design of third-order PLL. It is easy to design the PLL with desired specifications such as PM, damping ratio, natural frequency and small signal settling time using the proposed analytical equations. Also, validity of the proposed technique is verified by simulation of the PLL system in MATLAB. All simulation results show a very good precision in the designed parameters.

REFERENCES

- Carlосena A, Lazaro AM (2006). A Novel Design Method for Phased-Locked Loops of any Order and Type. IEEE MWSCAS: pp. 569-573.
- Carlосena A, Ugarte M, López-Martín AJ (2008). Loop Filter Approximation for PLLs. IEEE MWSCAS: pp. 21-24.
- Gardner FM (1980). Charge-Pump Phase-Lock Loops. IEEE Trans. Comm., 28(11): 1849-1858.
- Kim J, Shin J, Kim S, Shin H (2008). A Wide-Band CMOS LC VCO with Linearized Coarse Tuning Characteristic. IEEE Trans. Circuits Syst., 55(5): 399-403.
- Lakshmikumkar KR (2009). Analog PLL Design with Ring Oscillators at Low-Gigahertz in Nanometer CMOS: Challenges and Solutions. IEEE Trans. Circ. Syst., 56(5): 1549-1554.
- Monterio LAH, Favaretto DN, Filho J, Piqueira JRC (2004). Bifurcation Analysis for Third-Order Phased-Locked Loops. IEEE signal processing let., 1(5): 494-496.
- Nakamura T, Kitama T, Hayashi N (2006). A Wide-Tuning range VCO with Small VCO-gain Fluctuation for Multi-band W-CDMA. IEEE ESSCRIC: pp. 448-451.
- Ping-Hsuan H, Maxey J, Yang CK (2011). A Phase-Selecting Digital Phase-Locked Loop With Bandwidth Tracking in 65-nm CMOS Technology. IEEE J. Solid-State Circuits, 45(4): 781-792.
- Razavi B (2001). Design of Analog CMOS Integrated Circuits. New York. MacGraw-Hill.
- Woo K, Liu Y, Nam E, Ham D (2008). Fast-Lock Hybrid PLL Combining Fractional-N and Integer Modes of Differing Bandwidths. IEEE J. of Solid-State Circuits, 43(2): 379-389.
- Yin W, Inti R, Elshazly A, Young B, Hanumolu PK (2011). A 0.7-to-3.5 GHz 0.6-to-2.8 mW Highly Digital Phase-Locked Loop With Bandwidth Tracking. IEEE J. Solid-State Circuits, 46(8): 1870-1880.
- You F, He S (2004). Analysis of Third-order Charge Pump PLLs. IEEE ICCAS: pp.1372-1376.